JOURNAL OF SOLID STATE CHEMISTRY 115, 456–463 (1995)

The Effects of Substitution of Alkaline Earths or Y for La on Structure and Electrical Properties of $LaSrFeO_4$

Shinobu Fujihara, Toshiyuki Nakata, Hiromitsu Kozuka,[1] and Toshinobu Yoko

Institute for Chemical Research, Kyoto University, Uji, Kyoto-Fu 611, Japan

Received May 17, 1994; in revised form August 8, 1994; accepted August 12, 1994

The effects of the substitution of alkaline earths or Y for La on the structure and electrical properties of $LaSrFeO_4$ with K_2NiF_4 structure have been investigated. EDTA titration confirmed that Fe^{3+} was oxidized to Fe^{4+} in an amount corresponding to that of divalent alkaline earth ions substituted for La^{3+}. The change in the lattice constants was interpreted in terms of the ionic radius of the substituted ions and the Jahn–Teller distortion of the Fe(IV)O_6 octahedra having d^4 electronic configuration. All the substituted $LaSrFeO_4$ samples were semiconducting over the temperature range from 100 to 300 K. The measurement of the Seebeck coefficient revealed that the conduction carriers of $LaSrFeO_4$ were holes and the carrier concentration increased with increasing amount of Fe^{4+}. $La_{1-x}A_xSrFeO_4$ exhibited a monotonic decrease in resistivity and activation energy for conduction with increasing Fe^{4+} abundance. The activation energy for conduction did not change by changing the lattice constant where the Fe^{4+} abundance did not change with various substituents. © 1995 Academic Press, Inc.

1. INTRODUCTION

Since the discovery of high-temperature superconductivity in a series of copper oxide systems (1–3), perovskite-related 3*d* transition metal oxides have attracted renewed attention in understanding the mechanism of superconductivity and in the search for new superconductors. In particular, A_2BO_4 compounds (A, rare earth and/or alkaline earth and B, transition metal) with K_2NiF_4 structure have been the targets of intensive studies because of their structural similarity to the $La_{2-x}Sr_xCuO_4$ superconductor.

It is well known (4–6) that the properties of A_2BO_4 compounds change depending on the formal valence of transition metal ions and/or the lattice constants. The valence of B ions in A_2BO_4 is variable with ionic substitution at the A-site or with varying oxygen content, which often gives rise to the change in the lattice constants because of the interaction between the transition metal ions and oxygen ions. The change in the lattice constants without any change in the formal valence also affects the properties of A_2BO_4. The $La_{2-x}Sr_xCuO_4$ superconductor is the best example which exhibits all of these phenomena (4, 6, 7).

A series of $(La, Sr)_2FeO_4$ with K_2NiF_4 structure shows different electrical properties depending on the valence of iron and/or the La : Sr ratio. It was reported by King *et al.* (8) that at room temperature La_2FeO_4 with Fe^{2+} is insulating with a resistivity of $>10^7$ Ω cm, and $La_{1.5}Sr_{0.5}FeO_4$ with mixed Fe^{2+}/Fe^{3+} and $LaSrFeO_4$ with Fe^{3+} are semiconducting with a resistivity of 9.8×10^3 and 2.4×10^3 Ω cm, respectively. Although the exact valence of iron was not determined in their work, at least it seems that the resistivity of $(La, Sr)_2FeO_4$ decreases as the proportion of the higher oxidation state of iron in the La-rich compositions increases. Recently, we have studied the Sr-rich $La_{1-x}Sr_{1+x}FeO_4$ in the range $0 \le x \le 0.20$ (9). It was shown that the substitution of Sr^{2+} for La^{3+} results in the oxidation of Fe^{3+} to Fe^{4+} with the formation of holes, the concentration of which increases in proportion to x. As a result, the resistivity and the activation energy for conduction decrease, the lattice constant a decreases, and c increases with increasing x in $La_{1-x}Sr_{1+x}FeO_4$ (9). It is expected that the substitution of Ca or Ba for La in $LaSrFeO_4$ changes both the valence of iron and the lattice constants. The substitution of Y for La is expected to change the lattice constants without any change in the valence of Fe ions.

In the present paper, we report the effects of the substitution of alkaline earths (Ca, Sr, and Ba) or Y for La on the structure and electrical properties of $LaSrFeO_4$. Using polycrystalline samples of $La_{1-x}A_xSrFeO_4$ (A = Ca, Sr, Ba, $0 \le x \le 0.20$) and $La_{1-(x+y)}Y_ySr_{1+x}FeO_4$ ($x = 0.10$, $0 \le y \le 0.30$) prepared by solid-state reaction, changes in Fe^{3+}/Fe^{4+} ratio, lattice constants, and electrical properties with composition x and y and/or variation of substituents are investigated.

2. EXPERIMENTAL

$La_{1-x}A_xSrFeO_4$ (A = Ca, Sr, and Ba) and $La_{0.9-y}Y_ySr_{1.1}FeO_4$ were prepared by solid-state reaction. The

[1] To whom correspondence should be addressed.

0022-4596/95 $6.00
Copyright © 1995 by Academic Press, Inc.
All rights of reproduction in any form reserved.

oxide and carbonate powder reagents, La_2O_3 (99.99%, Wako Pure Chemical Industries, Osaka, Japan), Y_2O_3 (99.99%, Wako Pure Chemical Industries), $SrCO_3$ (99.5%, Nacalai Tesque, Kyoto, Japan), $CaCO_3$ (99.5%, Nacalai Tesque), $BaCO_3$ (99.5%, Nacalai Tesque), and Fe_2O_3 (98.0%, Wako Pure Chemical Industries) were used as starting materials. The mixtures of the chemicals in the desired atomic ratios were first calcined at 1000°C for 20 hr in air. The calcined powders were ground and pressed into pellets of 13 mm diameter and about 1 mm thick under a pressure of 60 kg/cm^2, heated at 1400°C for 20 hr in air, and cooled in the furnace to room temperature. The resultant pellets were annealed in flowing oxygen at 700°C for 50 hr. In order to avoid contamination from the supports during the heat treatment, the pellets were placed on calcined powders of the same composition, which were supported on a platinum plate.

The crystalline phases evolved in the samples after the heat treatment were identified by the powder X-ray diffraction method (XRD) with a Rigaku Denki Company Model RAD-IIA diffractometer using Cu$K\alpha$ radiation. The lattice constants of the $La_{1-x}A_xSrFeO_4$ (A = Ca, Sr, and Ba) and $La_{0.9-y}Y_ySr_{1.1}FeO_4$ crystals were determined by the XRD using Si as an internal standard substance.

The formal valence of Fe in single-phase $La_{1-x}A_xSrFeO_4$ was determined by EDTA titration (10). The pulverized sample (approximately 750 mg) was exactly weighed and dissolved in a 25-ml aqueous solution containing 1.5 ml of concentrated HCl and 283.7 mg of $FeCl_2$ (corresponding to 125 mg of Fe^{2+}) at 60°C while the solution was purged with CO_2 gas. Then the solution was cooled and diluted with CO_2-saturated water to 50 ml, 1 ml of which was added to a buffer solution consisting of 1 N HCl and 1 M CH_3COONa with a volume ratio of 1 : 1. After adding a few drops of 1% methanol solution of salicylic acid as indicator, the solution was titrated with 0.01 M EDTA standard solution to determine Fe^{3+} ions. Then, after adjusting the pH of the solution to 5 with an aqueous solution of hexamethylenetetramine and adding a 0.5% aqueous solution of methylthymol blue as an indicator, the resultant solution was placed in a water bath at 60°C and titrated with 0.01 M EDTA standard solution to determine the amount of Fe^{2+} ions. Representing the amount of the initially added Fe^{2+} by p and the determined Fe^{3+} and Fe^{2+} by q and r, respectively, the amount of Fe^{4+}, m, and Fe^{3+}, n, in the samples can be given as $m = p - r$ and $n = q + 2r - 2p$, since Fe^{4+} and Fe^{2+} react to form Fe^{3+} ($Fe^{4+} + Fe^{2+} \rightarrow 2Fe^{3+}$) in the solution.

The dc electrical resistivity of the samples was measured at temperatures from 100 to 300 K by the three-probe method (11). The electrodes were formed by evaporating Au onto the surface of the pellets and were connected to the leads with silver paste. The Seebeck coefficient of the $La_{1-x}Sr_{1+x}FeO_4$ samples was determined by measuring the electrical voltage produced between both ends of the pellet sample when one end of the sample was heated.

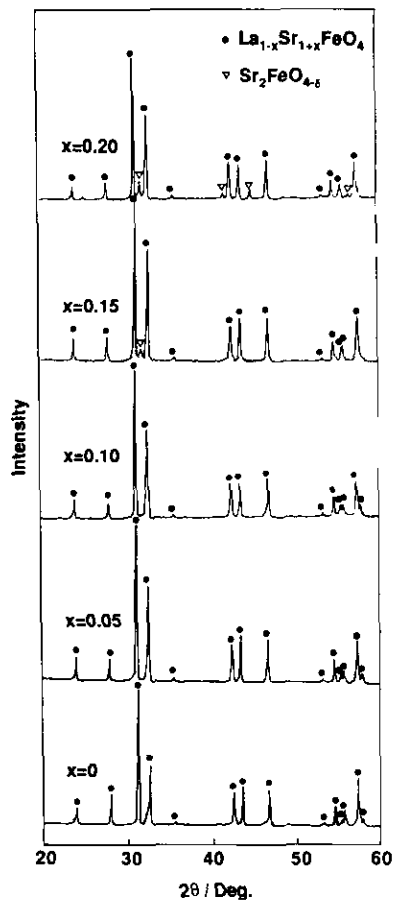

FIG. 1. X-ray diffraction patterns of $La_{1-x}Sr_{1+x}FeO_4$ in the range $0 \leq x \leq 0.20$ after heating at 1400° C for 20 hr in air.

3. RESULTS

3.1. X-Ray Diffraction Analysis

The XRD patterns of the heat-treated samples of $La_{1-x}Sr_{1+x}FeO_4$ ($0 \leq x \leq 0.20$) are shown in Fig. 1. In the range $0 \leq x \leq 0.10$, the patterns show a single phase of K_2NiF_4 structure with the tetragonal $I4/mmm$ space group symmetry. On the other hand, the samples of $x \geq 0.15$ contain $Sr_2FeO_{4-\delta}$ as a second phase, which did not disappear even when heat treatment at 1400°C was prolonged for up to 30 hr. The color of the samples changed from dark brown for $x = 0$ to black for $x = 0.05$ and 0.10.

The XRD patterns of the heat-treated samples of $La_{1-x}Ca_xSrFeO_4$ and $La_{1-x}Ba_xSrFeO_4$ ($x = 0.10$, 0.15) are shown in Fig. 2. The patterns of both the Ca- and Ba-substituted samples of $x = 0.10$ show a single phase of the tetragonal $I4/mmm$ K_2NiF_4 structure. The samples of

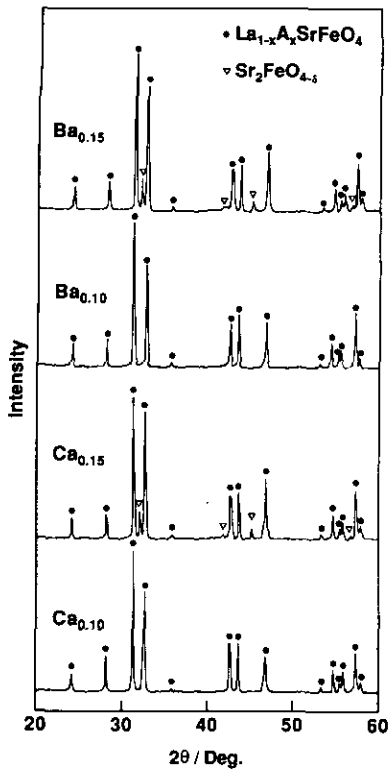

FIG. 2. X-ray diffraction patterns of $La_{1-x}Ca_xSrFeO_4$ and $La_{1-x}Ba_xSrFeO_4$ at $x = 0.10$ and 0.15 after heating at 1400°C for 20 hr in air.

$x = 0.15$ with Ca and Ba substitution contain $Sr_2FeO_{4-\delta}$ as a second phase, as in the case of the $La_{1-x}Sr_{1+x}FeO_4$ samples.

The XRD patterns of the heat-treated samples of $La_{0.9-y}Y_ySr_{1.1}FeO_4$ in the range $0.10 \leq y \leq 0.30$ are shown in Fig. 3. The patterns of the samples of $y = 0.10$ and 0.20 show a single phase of tetragonal *I4/mmm* K_2NiF_4 structure, whereas the sample of $y = 0.30$ contains a trace of Y_2O_3 as an impurity phase.

3.2. Fe^{3+}/Fe^{4+} Ratio and Oxygen Content

The relative abundance (%) of Fe^{3+} and Fe^{4+} of the single phase $La_{1-x}A_xSrFeO_4$ ($x = 0$, 0.05, 0.10 for A = Sr and $x = 0.10$ for A = Ca, Ba) samples are summarized in Table 1. The abundance of Fe^{4+} increases from 0.9 to 4.7 to 10.2% with increasing x from 0 to 0.05 to 0.1 in $La_{1-x}Sr_{1+x}FeO_4$. The abundance of Fe^{4+} of the Ca- and Ba-substituted samples with $x = 0.10$ are 8.7 and 9.6%, respectively. The measured abundance of Fe^{4+} in $La_{1-x}A_xSrFeO_4$ is in excellent agreement with the calculated one indicating that all the added divalent alkaline earth ions are substituted for trivalent La.

The oxygen content was calculated from the measured Fe^{3+} and Fe^{4+} abundances and the nominal composition, assuming that La, alkaline earths and O have the formal valence of +3, +2 and −2, respectively. The oxygen contents of all the single phase $La_{1-x}Sr_{1+x}FeO_4$ samples are calculated to be 4.00 and those of $La_{0.9}Ca_{0.1}SrFeO_4$ and $La_{0.9}Ba_{0.1}SrFeO_4$ to be 3.99 and 4.00, respectively. These results indicate that the present ionic substitution does not cause the oxygen defect formation.

3.3. Lattice Constants

The lattice constants a and c of the $La_{1-x}A_xSrFeO_4$ samples are plotted against x in Fig. 4 and summarized in Table 1. The experimental error of these values is within 0.05%. The lattice constants of the parent $LaSrFeO_4$ obtained in the present work, $a = 0.3876$ nm and $c = 1.2713$ nm, agree well with those reported by Shimada and Koizumi (12). As seen in Fig. 4, the lattice constant a decreases while c increases monotonically with increasing x in $La_{1-x}Sr_{1+x}FeO_4$. The rate of their change with x from 0 to 0.10 is 0.21% for a and 0.19% for c. In the range $x > 0.10$, where the samples contain impurity phases, the change in the lattice constants becomes smaller, which is partially because of the imperfect solubility of Sr in the compound for $x > 0.10$.

Both of the lattice constants a and c decrease monotonically with increasing x in $La_{1-x}Ca_xSrFeO_4$. In contrast, the lattice constant a is nearly constant and c increases with increasing x in $La_{1-x}Ba_xSrFeO_4$. The rate of decrease in the lattice constant a for the Ca-substituted sample is 0.21% in the range $0 \leq x \leq 0.10$. The rate of change in the lattice constant c is 0.18% (decrease) for the Ca and 0.29% (increase) for the Ba-substituted sample in the range $0 \leq x \leq 0.10$.

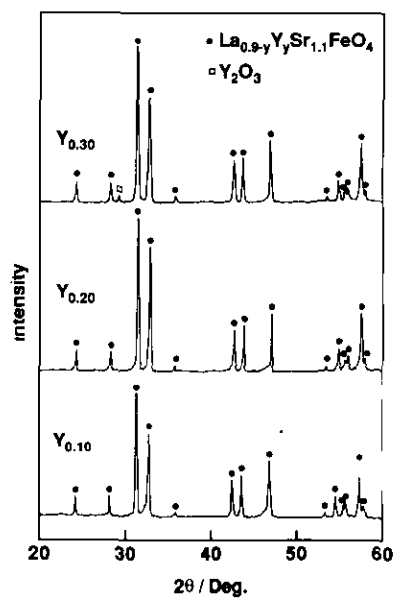

FIG. 3. X-ray diffraction patterns of $La_{0.9-y}Y_ySr_{1.1}FeO_4$ in the range $0.10 \leq y \leq 0.30$ after heating at 1400°C for 20 hr in air.

TABLE 1

Abundance of Fe^{3+} and Fe^{4+}, Oxygen Content, Lattice Constants, Resistivity ρ, Activation Energy for Electrical Conduction E_a, and Seebeck Coefficient Q of the Parent $LaSrFeO_4$ and the Substituted $La_{1-x}A_xSrFeO_4$ (A = Sr, Ca, and Ba) and $La_{0.9-y}Y_ySr_{1.1}FeO_4$ Samples

Sample (A_x, Y_y)	Abundance (%)		Oxygen content	Lattice constants (nm)		ρ (Ω cm)	E_a (eV)	Q (mV K^{-1})
	Fe^{3+}	Fe^{4+}		a	c			
$LaSrFeO_4$	99.1	0.9	4.00	0.3876	1.2713	1.15×10^5	0.338	0.175
$Sr_{0.05}$	95.3	4.7	4.00	0.3873	1.2720	2.21×10^3	0.306	0.152
$Sr_{0.10}$	89.8	10.2	4.00	0.3868	1.2737	6.81×10^2	0.281	0.141
$Sr_{0.15}$[a]	—	—	—	0.3866	1.2745	—	—	—
$Sr_{0.20}$[a]	—	—	—	0.3865	1.2743	—	—	—
$Ca_{0.10}$	91.3	8.7	3.99	0.3868	1.2690	6.72×10^2	0.276	0.147
$Ca_{0.15}$[a]	—	—	—	0.3867	1.2684	—	—	—
$Ba_{0.10}$	90.4	9.6	4.00	0.3875	1.2750	8.99×10^1	0.276	0.140
$Ba_{0.15}$[a]	—	—	—	0.3876	1.2761	—	—	
$Y_{0.10}$	—	—	—	0.3864	1.2704	—	0.289	—
$Y_{0.20}$	—	—	—	0.3861	1.2673	—	—	0.155

[a] Not a single phase with K_2NiF_4 structure.

The lattice constants a and c of the $La_{0.9-y}Y_ySr_{1.1}FeO_4$ samples are summarized in Table 1. Figure 5 shows the change in the lattice constants of $La_{1-(x+y)}Y_ySr_{1+x}FeO_4$ with x and y in the range $0 \leq x \leq 0.10$ at $y = 0$ and $0.10 \leq y \leq 0.20$ at $x = 0.10$. It is seen that the lattice constant a, which decreases with increasing x in $La_{1-x}Sr_{1+x}FeO_4$ from 0 to 0.10, continues to decrease with increasing y in $La_{0.9-y}Y_ySr_{1.1}FeO_4$ from 0 to 0.20. On the contrary, the lattice constant c, which increases with x, turns to decrease with increasing y in the range $0 \leq y \leq 0.20$. The rate of decrease in the lattice constants is 0.18% for a and 0.50% for c with increasing y from 0 to 0.20.

3.4. Electrical Properties

As summarized in Table 1, the resistivity of $La_{1-x}Sr_{1+x}FeO_4$ at 300 K was 1.15×10^5 Ω cm for $x = 0$, 2.21×10^3 Ω cm for $x = 0.05$, and 6.81×10^2 Ω cm for $x = 0.10$, which shows a monotonical decrease with increasing x. The resistivity of $La_{0.9}Ca_{0.1}SrFeO_4$ and $La_{0.9}Ba_{0.1}SrFeO_4$ at 300 K was 6.72×10^2 and 8.99×10^1 Ω cm, respectively.

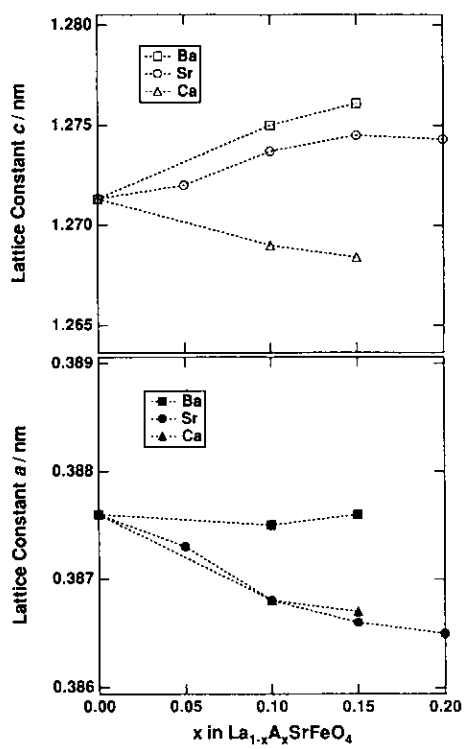

FIG. 4. Variation of the lattice constants a and c as a function of x in a series of $La_{1-x}A_xSrFeO_4$.

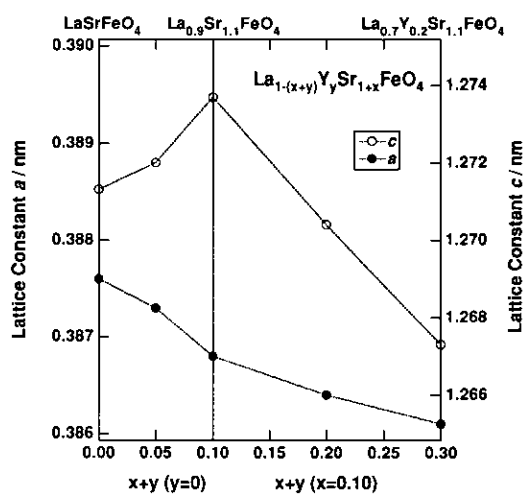

FIG. 5. Variation of the lattice constants a and c as a function of x and y in a series of $La_{1-(x+y)}Y_ySr_{1+x}FeO_4$.

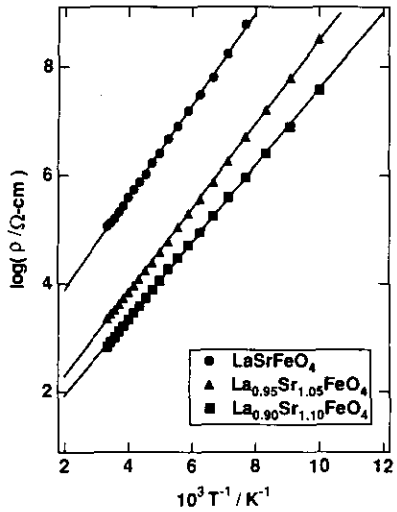

FIG. 6. Log ρ vs $1/T$ plot in $La_{1-x}Sr_{1+x}FeO_4$ with $x = 0$, 0.05, and 0.10.

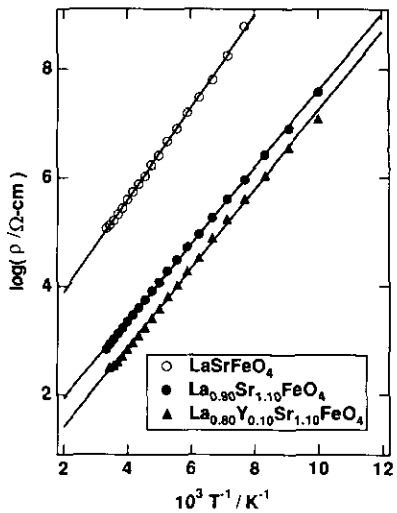

FIG. 8. Log ρ vs $1/T$ plot in $La_{0.9-y}Y_ySr_{1.1}FeO_4$ with $y = 0$ and 0.10.

Figures 6, 7, and 8 show Arrhenius plots of log ρ vs $1/T$, where ρ is the resistivity and T is the absolute temperature, for the series $La_{1-x}Sr_{1+x}FeO_4$, $La_{0.9}A_{0.1}SrFeO_4$ (A = Ca, Sr, Ba), and $La_{0.9-y}Y_ySr_{1.1}FeO_4$, respectively. Temperature dependences of the resistivity for all the samples indicate semiconducting behavior with $d\rho/dT < 0$.

Since straight lines have been given by an Arrhenius plot in the temperature range employed in the present measurement as seen in Figs. 6, 7, and 8, the apparent activation energy for conduction of the samples, E_a, can be calculated from the plot using

$$\ln \rho = E_a/2k_BT + C, \qquad [1]$$

where k_B is the Boltzmann constant and C is a constant. The E_a values are summarized in Table 1 and those of the $La_{1-x}Sr_{1+x}FeO_4$ and $La_{0.9}A_{0.1}SrFeO_4$ samples are plotted against x and the kinds of A, respectively, in Figs. 9a and 9b. It is seen that E_a decreases monotonically with increasing x in $La_{1-x}Sr_{1+x}FeO_4$. On the other hand, the value of E_a hardly depends on the kinds of alkaline earths in $La_{0.9}A_{0.1}SrFeO_4$.

The Seebeck coefficient Q was determined from (13)

$$Q = \frac{dV}{dT} = -\frac{V_h - V_c}{T_h - T_c}, \qquad [2]$$

where $V_h - V_c$ and $T_h - T_c$ are the electromotive force and temperature difference between the hot and cold ends of the sample, respectively. The values of the Seebeck coefficient Q of the samples are summarized in Table 1. All the

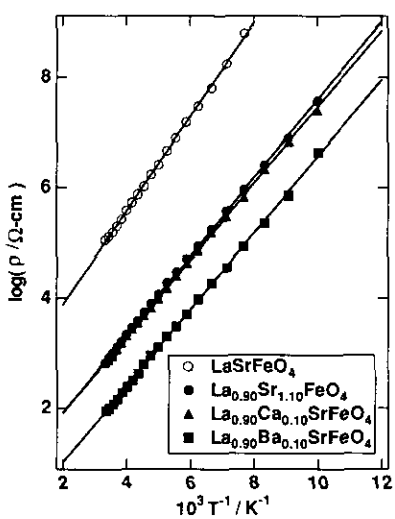

FIG. 7. Log ρ vs $1/T$ plot in $La_{0.9}A_{0.1}SrFeO_4$ with A = Ca, Sr, and Ba.

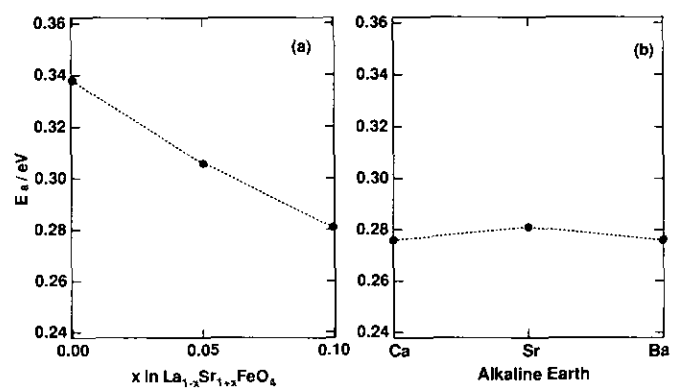

FIG. 9. Dependence of the activation energy for conduction (a) on x in $La_{1-x}Sr_{1+x}FeO_4$ and (b) on the kind of the alkaline earth metals.

Q values are positive. In $La_{1-x}Sr_{1+x}FeO_4$, Q decreases monotonically with increasing x.

4. DISCUSSION

4.1. Changes in the Lattice Constants by Ionic Substitution

The decrease in the lattice constant a with increasing x as observed in $La_{1-x}Sr_{1+x}FeO_4$ cannot be explained by the difference in ionic radius between La^{3+} and Sr^{2+} since Sr^{2+} has a larger ionic radius (0.131 nm) than La^{3+} (0.1216 nm) (14). An interpretation can be made on the basis of the electronic state of the Fe ions and the crystal structure featured by two-dimensionally linked FeO_6 octahedra. The FeO_6 octahedra containing Fe^{3+} ions in the parent $LaSrFeO_4$ do not undergo Jahn–Teller distortion because they have five $3d$ electrons in a high-spin state (15), three of which lie in lower t_{2g} orbitals and two of which lie in higher e_g orbitals. However, when one electron is removed from the e_g orbital of Fe^{3+} ion to form Fe^{4+}, and the introduced hole and the other retained e_g electron are localized at the Fe^{4+} ion, the $Fe(IV)O_6$ octahedron should undergo Jahn–Teller distortion with contraction in the x–y plane and expansion in the z direction. The decrease in the lattice constant a and the increase in c observed in $La_{1-x}Sr_{1+x}FeO_4$ with increasing x are thus considered to be caused by the Jahn–Teller distortion of the FeO_6 octahedra. The localization of holes on the Fe ions is likely to occur in the K_2NiF_4 structure featured by the strong two-dimensionality, in contrast to the three-dimensional perovskite $SrFeO_3$, which does not exhibit Jahn–Teller distortion because of the itinerant nature of e_g electrons (16).

The rate of decrease in the lattice constant a as observed in $La_{1-x}Ca_xSrFeO_4$ is much larger than expected from the slightly smaller ionic radius of Ca^{2+} (0.118 nm) than La^{3+} (0.1216 nm). This is also thought to result from the distorted FeO_6 octahedra by Jahn–Teller effect. Little change in the lattice constant a in $La_{1-x}Ba_xSrFeO_4$ may be attributed to the compensating effects of the larger ionic radius of Ba^{2+} (0.147 nm) and Jahn–Teller distortion, which would expand and contract the a-axis, respectively.

In contrast to the lattice constant a, the decrease in the lattice constant c with increasing x in $La_{1-x}Ca_xSrFeO_4$ and the increase in $La_{1-x}Sr_{1+x}FeO_4$ and $La_{1-x}Ba_xSrFeO_4$ can be appropriately explained by the differences in the ionic radius of the alkaline earths. Because $LaSrFeO_4$ is composed of two (La, Sr)O and one FeO_2 layers stacked alternately along the c-axis, the size of the cations in the (La, Sr)O layers is expected to affect more significantly the lattice constant c than the lattice constant a. That is, larger ions such as Sr^{2+} and Ba^{2+} that are substituted for La^{3+} elongate the interlayer distance while smaller ions such as Ca^{2+} shorten it, which results in the observed change in the lattice constant c.

A comparison of the three samples of $La_{0.9}A_{0.1}SrFeO_4$ (A = Ca, Sr, Ba), which differ only in the kind of alkaline earth, exhibits clearly the effect of the ionic radius on the structure. The lattice constants a and c show a 0.18 and 0.47% increase, respectively, with increasing ionic radius from 0.118 (Ca^{2+}) to 0.147 nm (Ba^{2+}). The smaller rate of increase in a is possibly due to the stiff Fe–O bond in the two-dimensional FeO_2 planes, which makes the lattice constant a difficult to change. In contrast, the larger rate of increase in c reflects that the lattice constant c easily changes by the substitution of ions with different ionic radii.

As shown in Fig. 5, the decrease in the lattice constants a and c in $La_{0.9-y}Y_ySr_{1.1}FeO_4$ on changing y from 0 to 0.20 is thought to result principally from the smaller ionic radius of Y^{3+} (0.1075 nm) than La^{3+} (0.1216 nm) because the substitution of Y^{3+} for La^{3+} does not cause the valence change of Fe which affects the electronic structure. The rate of decrease in the lattice constants is 0.18% for a and 0.50% for c as y increases from 0 to 0.20. Such a difference can be also interpreted by the same reasoning as mentioned above.

4.2. Changes in the Electrical Properties by Ionic Substitution

The $La_{1-x}Sr_{1+x}FeO_4$ samples were found to exhibit semiconducting behavior and their resistivity decreased with increasing x. The activation energy for conduction E_a showed a monotonical decrease with increasing x. The sign of the charge carrier and the change in the carrier concentration can be determined from the Seebeck coefficient (13). When the electrical conductivity is ascribed to a single kind of carrier (13), the Seebeck coefficient Q is expressed by

$$Q = \pm\frac{k_B}{e}\left(\frac{E_F}{k_BT} + A\right) = \pm\frac{k_B}{e}\left(\ln\frac{N}{c} + A\right), \qquad [3]$$

where E_F is the energy gap between the Fermi level and the transport level, bottom of the conduction band (n-type), or top of the valence band (p-type), A is the energy transport term, N is the effective density of states at the transport level, and c is the carrier concentration. The observed positive Q values indicate that the conduction carriers in the present $La_{1-x}Sr_{1+x}FeO_4$ samples are holes. The observation that Q decreases with x suggests that the number of carriers increases with increasing x. In other words, the number of holes increases with increasing Fe^{4+} formed by charge compensation in substituting Sr^{2+} for La^{3+}. It can be concluded, therefore, that the decrease in the resistivity of $La_{1-x}Sr_{1+x}FeO_4$ with increasing x results

from the increase in the carrier concentration and the decrease in the activation energy for conduction. Adler (17) has studied quite recently the properties of the K_2NiF_4-type $Sr_2FeO_{4-\delta}$, which corresponds to the composition of $x = 1$ in $La_{1-x}Sr_{1+x}FeO_4$, with 88% of Fe^{4+} in abundance. According to his report, $Sr_2FeO_{4-\delta}$ exhibits semiconducting behavior and has the activation energy E_a of 0.18 eV, which is smaller than those of the present $La_{1-x}Sr_{1+x}FeO_4$ samples (0.338 eV for $x = 0$ and 0.281 eV for $x = 0.10$). It can be expected, therefore, that $La_{1-x}Sr_{1+x}FeO_4$ will exhibit semiconducting behavior and E_a will continue to decrease with increasing Fe^{4+} content in the whole range of x.

The change in the activation energy for conduction E_a of $LaSrFeO_4$ by the substitution is considered to result from the change in the electronic structure around the Fermi level, which is composed of the Fe-$3d_{x^2-y^2}$ and O-$2p_\sigma$ bands. Since the Fe-$3d_{x^2-y^2}$ and O-$2p_\sigma$ are the x–y components of the bands, the Fe–O distance and angle in the FeO_2 planes, which determine the lattice constant a, are thought to affect the band structure. The decrease in E_a with increasing x observed in $La_{1-x}Sr_{1+x}FeO_4$, therefore, is expected to result from the change in electronic structure due to the decrease in the lattice constant a as well as the increase in the number of holes in the Fe-$3d_{x^2-y^2}$ or O-$2p_\sigma$ bands. E_a values of the three $La_{0.9}A_{0.1}SrFeO_4$ (A = Ca, Sr, Ba) samples, however, were hardly dependent on the kind of alkaline earths, although the lattice constant a of $La_{0.9}Ba_{0.1}SrFeO_4$ (0.3875 nm) is larger than that of $La_{0.9}Ca_{0.1}SrFeO_4$ (0.3868 nm) and $La_{0.9}Sr_{1.1}FeO_4$ (0.3868 nm). In addition, E_a values of the $La_{0.9-y}Y_ySr_{1.1}FeO_4$ samples are also almost unchanged with increasing y, as shown in Table 1, although the lattice constant a decreases monotonically with increasing y. It is thought, in consequence, that the change in the lattice constant a (0.18%) attained in the presently studied $La_{0.9}A_{0.1}SrFeO_4$ and $La_{0.9-y}Y_ySr_{1.1}FeO_4$ is too small to change the electronic structure and accordingly the activation energy for conduction. Thus the decrease in E_a with increasing x in $La_{1-x}Sr_{1+x}FeO_4$ is ascribed to the change in the electronic structure mainly due to the increase in the hole concentration. The large increase in the lattice constant c (0.47% for $La_{0.9}A_{0.1}SrFeO_4$ and 0.50% for $La_{0.9-y}Y_ySr_{1.1}FeO_4$) does not affect the activation energy, which is easily expected from the two-dimensional feature of the electronic structure around the Fermi level in the x–y plane as mentioned above.

The resistivities of the three $La_{0.9}A_{0.1}SrFeO_4$ samples, 6.72×10^2, 6.81×10^2, and 8.99×10^1 Ω cm for $La_{0.9}Ca_{0.1}SrFeO_4$, $La_{0.9}Sr_{1.1}FeO_4$, and $La_{0.9}Ba_{0.1}SrFeO_4$, respectively, correspond neither to the change in the activation energy for conduction, which is independent of the kind of alkaline earths as shown in Fig. 9b, nor to that in the Seebeck coefficient, which is almost constant as shown in Table 1.

5. CONCLUSION

The formation, lattice constants, and electrical properties of the $LaSrFeO_4$ system with substitution of alkaline earths or Y for La were studied, and the following results were obtained.

1. Single-phase compounds with the K_2NiF_4 structure were obtained in the range $0 \le x \le 0.10$ and $0 \le y \le 0.20$ for $La_{1-x}A_xSrFeO_4$ (A = Ca, Sr, Ba) and $La_{0.9-y}Y_ySr_{1.1}FeO_4$, respectively.

2. From the EDTA titration, it was shown that Fe^{3+} was oxidized to Fe^{4+} in an amount corresponding to the substituted alkaline-earth ion amounts, resulting in an Fe^{3+}/Fe^{4+} mixed valence state.

3. The lattice constant a decreased monotonically with increasing x for A = Ca and Sr and was almost unchanged for A = Ba, whereas c decreased with increasing x for A = Ca and increased for A = Sr and Ba. In $La_{0.9-y}Y_ySr_{1.1}FeO_4$, both the lattice constants a and c decreased with increasing y.

4. The electrical conductivity of all the substituted $LaSrFeO_4$ samples was semiconducting in the temperature range 100–300 K, and the resistivity decreased with increasing Fe^{4+}, which was considered to result from the increase in the carrier concentration, as evidenced by the Seebeck coefficient measurement and the decrease in the activation energy.

5. The activation energy for conduction decreased with increasing x or with increasing Fe^{4+} in $La_{1-x}Sr_{1+x}FeO_4$. The change in the lattice constant a without changing the Fe^{4+} content, however, did not cause the change in the activation energy in the present samples.

REFERENCES

1. J. G. Bednorz and K. A. Müller, *Z. Phys. B* **64,** 189 (1986).
2. M. K. Wu, J. R. Ashburn, C. J. Torng, P. H. Hor, R. L. Meng, L. Gao, Z. J. Huang, Y. Q. Wang, and C. W. Chu, *Phys. Rev. Lett.* **58,** 908 (1987).
3. H. Maeda, Y. Tanaka, M. Fukutomi, and T. Asano, *Jpn. J. Appl. Phys.* **27,** L209 (1988).
4. J. B. Torrance, Y. Tokura, A. I. Nazzal, A. Bezinge, T. C. Huang, and S. S. P. Parkin, *Phys. Rev. Lett.* **61,** 1127 (1988).
5. C. J. Liu, M. D. Mays, D. O. Cowan, and M. G. Sánchez, *Chem. Mater.* **3,** 495 (1991).
6. K. Kishio, K. Kitazawa, N. Sugii, S. Kanbe, K. Fueki, H. Takagi, and S. Tanaka, *Chem. Lett.*, 635 (1987).
7. J. G. Bednorz, M. Takashige, and K. A. Müller, *Mater. Res. Bull.* **22,** 819 (1987).
8. H. W. King, K. M. Castelliz, G. J. Murphy, and A. S. Rizkalla, *J. Can. Ceram. Soc.* **55,** 10 (1986).

9. S. Fujihara, T. Nakata, H. Kozuka, and T. Yoko, submitted for publication.
10. S. Mori, H. Hirata, and N. Tonooka, *Jpn. Analyst* **16,** 1340 (1967).
11. R. N. Blumenthal and M. A. Seitz, "Electrical Conductivity in Ceramics and Glass, Part A" (N. M. Tallan, Ed.), p. 95. Dekker, New York, 1974.
12. M. Shimada and K. Koizumi, *Mater. Res. Bull.* **11,** 1237 (1976).
13. I. Bransky and N. M. Tallan, "Physics of Electronic Ceramics, Part A" (L. L. Hench and D. B. Dove, Eds.), p. 67. Dekker, New York, 1971.
14. R. D. Shannon, *Acta Crystallogr. Sect. A* **32,** 751 (1976).
15. K. K. Singh, P. Ganguly, P. P. Edwards, and J. B. Goodenough, *J. Phys. Condens. Matter* **3,** 2479 (1991).
16. M. Takano, N. Nakanishi, Y. Takeda, S. Naka, and T. Takada, *Mater. Res. Bull.* **12,** 923 (1977).
17. P. Adler, *J. Solid State Chem.* **108,** 275 (1994).